

# CRITICAL FIELDS OF SRF MATERIALS \*

T. Junginger<sup>†</sup>, Lancaster University, Bailrigg, Lancaster LA1 4YW, United Kingdom  
 The Cockcroft Institute, Daresbury, Warrington WA4 4AD, United Kingdom  
 T. Prokscha, Z. Salman, A. Suter Paul Scherrer Institut (PSI)  
 A-M. Valente-Feliciano Thomas Jefferson National Accelerator Facility (JLab)

## Abstract

Nb<sub>3</sub>Sn and NbTiN are two potential alternative materials to niobium for superconducting RF cavities. In this study direct measurements of the magnetic penetration depth using the low energy muon spin rotation technique are presented, from which the lower critical field and the superheating field are derived. Comparison with RF data confirms that the lower critical field is not a fundamental limitation and predict a potential performance clearly exceeding current state of the art of niobium technology if the superheating field can be achieved. As a potential pathway to avoid premature vortex penetration and reaching the superheating field it is suggested to use a bilayer structure with the outer layer having a larger magnetic penetration depth.

## INTRODUCTION

The material of choice for superconducting cavities is currently niobium, which is the material with the highest lower critical field  $H_{c1}$ . In order to achieve accelerating gradients beyond niobium technology it is necessary to operate cavities either in a mixed state with fluxoids in the material or in a metastable state above  $H_{c1}$ . The former solution would require strong pinning to avoid dissipation from vortices. The latter scenario can either be achieved by an energy barrier for vortex penetration or operating the cavities at a frequency which exceeds the time required for vortex penetration.

In this paper we present direct measurements of the London penetration depth of Nb<sub>3</sub>Sn and NbTiN using the low energy muon spin rotation technique. From these measurements we derive the lower critical field  $H_{c1}$ , the critical thermodynamic field  $H_c$  and the superheating field  $H_{sh}$ . (Table 1).

## METHOD

At PSI a low energy muon beam is available [1, 2]. It can be used as a probe for local magnetism at various depths between a few and up to about 300 nm depending on the material density. Applying a field below  $H_{c1}$  this allows to measure the local field  $H_{int}$  as a function of depth by varying the muon energy and therefore the implantation depth. This enables a direct measurement of the magnetic penetration depth  $\lambda$ . Results from two samples are presented here. A NbTiN film has been deposited by reactive DC magnetron sputtering at JLAB [3] while Nb<sub>3</sub>Sn was deposited using vapour diffusion at Cornell [4]. Substrates are made

\* This research was supported by a Marie Curie International Outgoing Fellowship within the EU Seventh Framework Programme for Research and Technological Development (2007-2013).

<sup>†</sup> Tobias.Junginger@lancaster.ac.uk

of RRR niobium<sup>1</sup> in both cases. Fig. 1 displays a transmission electron microscope image of the cross section of the NbTiN sample including a High Angle Annular Dark Field (HAADF) image. There is a well defined interface between the two materials and thickness of the NbTiN film is about  $d=160$  nm.

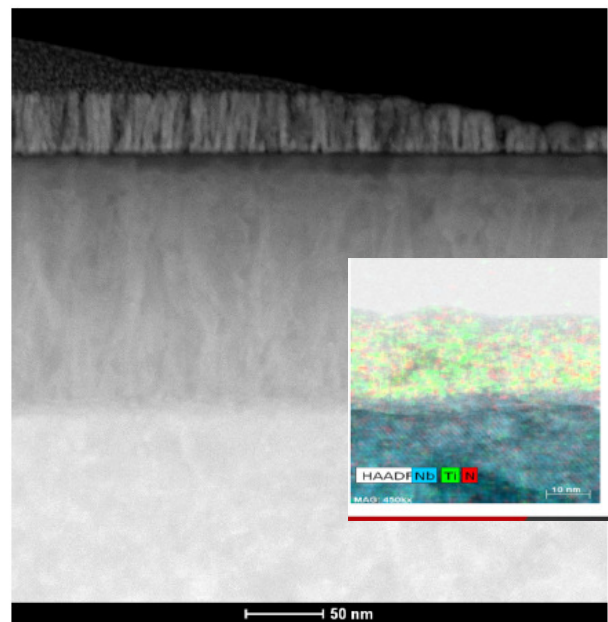


Figure 1: Transmission electron microscopy image of the cross section of a NbTiN on Nb sample from which the thickness of the sample is obtained. The uppermost layer is Pt added for protection for ion beam cutting. The inset shows a High Angle Annular Dark Field (HAADF) image revealing the elemental composition at the interface between the two materials.

## RESULTS

Figure 2 displays the internal magnetic field  $B_{int}$  as a function of mean muon implantation depth  $\langle x \rangle$  calculated with the muSRfit software [5] and the muon stopping distribution for NbTiN calculated with the TRIM.SP software [6] for the two samples. The thickness of Nb<sub>3</sub>Sn is about 2  $\mu$ m. This is large compared to the penetration depth  $\lambda$ , which can therefore be simply calculated from

$$B = B_0 \exp(-\langle x \rangle / \lambda) \quad (1)$$

<sup>1</sup> Niobium with a RRR > 300 is usually used for cavity fabrication and simply referred to as RRR niobium.

Table 1: Material parameters from literature and from our measurements. The upper estimate for  $\lambda_L$  of NbTiN is taken from our  $\lambda$  measurements.

Material	$\lambda_L$ [nm]	$\xi_0$ [nm]	$\lambda$ [nm]	$\kappa$	$H_{c1}$ [mT]	$H_c$ [mT]	$H_{sh}$ [mT]
Nb3Sn	65 [7]-89 [8]	5.7(0.6) [9]	160(4)	60(15)	28(2)	600(100)	410(70)
NbTiN	150 [10]-170	2.4(0.4) [11]	160(10)	70(16)	24(4)	500(200)	439(80)

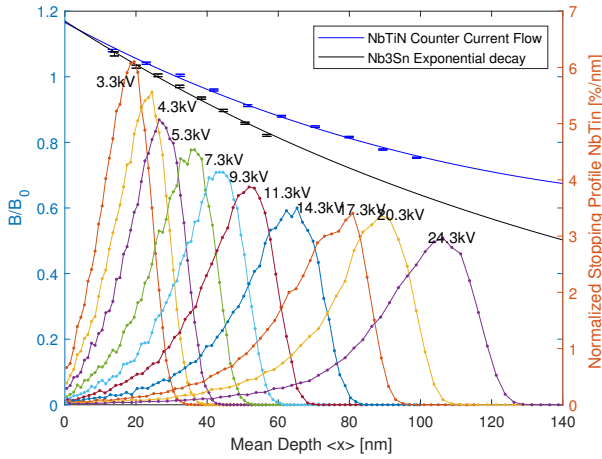


Figure 2: Normalized local magnetic field in the Nb3Sn and NbTiN samples as a function of mean muon implantation depth  $\langle x \rangle$  measured with low energy muon spin rotation. On the right y-axis the stopping profile for NbTiN is displayed.

where  $\langle x \rangle$  is the mean implantation depth of the muons. The fit parameters found are  $B_0=11.4$  mT and  $\lambda(5K)=160.5(3.9)$  nm.  $\lambda$  is expected to change according to

$$\lambda(T) = \frac{\lambda(0K)}{\sqrt{1 - (T/T_c)^4}}, \quad (2)$$

from which  $\lambda(0K)=160.0(3.9)$  nm can be derived. The value of  $B_0$  is 14 % larger than the applied field of 10 mT. This field enhancement is close to what is expected at the edge of the sample with demagnetization factor  $N=0.15$  [12]. The NbTiN film is so thin that counter current flow between film and substrate need to be considered [13, 14]. The penetration depth of the NbTiN layer  $\lambda_{NbTiN}$  is thus calculated using

$$B = B_0 \frac{\cosh \frac{d-\langle x \rangle}{\lambda_{NbTiN}} - \frac{\lambda_{Nb}}{\lambda_{NbTiN}} \sinh \frac{d-\langle x \rangle}{\lambda_{NbTiN}}}{\cosh \frac{d}{\lambda_{NbTiN}} - \frac{\lambda_{Nb}}{\lambda_{NbTiN}} \sinh \frac{d}{\lambda_{NbTiN}}} \quad (3)$$

where  $\lambda_{Nb}$  is the penetration depth of the Nb substrate which can be estimated to be 30-50 nm.  $\lambda_{NbTiN}(0K)=160(10)$  nm is derived which is significantly smaller to what one would calculate from Eq. 1 (233 nm). To obtain the Ginzburg Landau parameter  $\kappa = \lambda/\xi_{GL}$  from the measured value of  $\lambda$  one has to know the Ginzburg-Landau coherence length  $\xi_{GL}$  which is a property dependent on the material purity and can therefore not directly be obtained from literature. The fact that the BCS and the Ginzburg-Landau coherence length  $\xi_0$

and  $\xi_{GL}$  are both correlated to the magnetic flux quantum  $\Phi_0$  can be used to derive [15, 16]

$$\kappa = \frac{\lambda}{\xi_{GL}} = \frac{2\sqrt{3}}{\pi} \frac{\lambda^2}{\xi_0 \lambda_L}. \quad (4)$$

$\lambda_L$  and  $\xi_0$  are both fundamental properties which do not depend on purity. Literature values can be found in Tab. 1. Now the lower critical field  $H_{c1}$  can be derived from [16]

$$H_{c1} = \frac{\Phi_0}{\pi \lambda^2} \ln(\kappa + 0.5), \quad (5)$$

where  $\Phi_0$  is the magnetic flux quantum. From this the thermodynamic critical field can be calculated using [16]

$$H_c = \frac{\sqrt{2} \kappa H_{c1}}{\ln \kappa}. \quad (6)$$

The value for Nb3Sn (Tab. 1) is consistent with 530 mT reported in [8]. Finally the superheating field can be calculated using [17]

$$H_{sh} = H_c \left( \frac{\sqrt{20}}{6} - \frac{0.55}{\sqrt{\kappa}} \right). \quad (7)$$

The values, see Tab. 1 significantly exceed the superheating field of niobium (about 240 mT).

## DISCUSSION

The results predict superheating fields about twice as high as for Nb for both materials. However, the RF performance of Nb3Sn and NbTiN cavities is limited to surface magnetic fields significantly below  $H_{sh}$  but well above  $H_{c1}$  [18]. The obtained temperature dependence in such tests was found to be consistent with an heuristic model called vortex line nucleation which gives an estimate for the maximum RF field as

$$H_{VNL} = \frac{1}{\kappa} H_c. \quad (8)$$

However, the values of  $\kappa$  derived here would yield  $H_{VNL}$  well below  $H_{c1}$  and experimentally observed critical RF fields. On the other hand this model has given predictions for Nb in agreement with  $\kappa$  derived from low field surface impedance measurements [19]. This can be interpreted that the limitation of Nb3Sn and NbTiN, unlike for Nb, is not related to defects of the size of the coherence length on otherwise clean material with material parameters as displayed in Tab. 1.

Content from this work may be used under the terms of the CC BY 3.0 licence (© 2018). Any distribution of this work must maintain attribution to the author(s), title of the work, publisher, and DOI.

## HOW TO REACH LARGE ACCELERATING GRADIENTS

Several approaches have been suggested to reach accelerating gradients beyond the current state of the art with new materials. Defect free surfaces would allow to reach the superheating field. As Nb is operated in a metastable state above  $H_{c1}$  this might actually be possible to achieve for other materials as well. However, the coherence length of Nb is about ten times larger than for promising alternative materials such as NbTiN and Nb3Sn. To prevent flux penetration above  $H_{c1}$  Gurevich suggested to use alternating layers of superconductors and insulators, since there are no thermodynamically stable parallel vortices in decoupled layers which are thinner than the penetration depth [20]. A superconductor exposed to an RF field will remain in a flux free state above  $H_{c1}$  if the time it takes for flux to penetrate exceeds the RF period [21]. It might therefore be possible to engineer the outer surface to retard flux penetration as has recently been suggested by Romanenko [22]. On the other

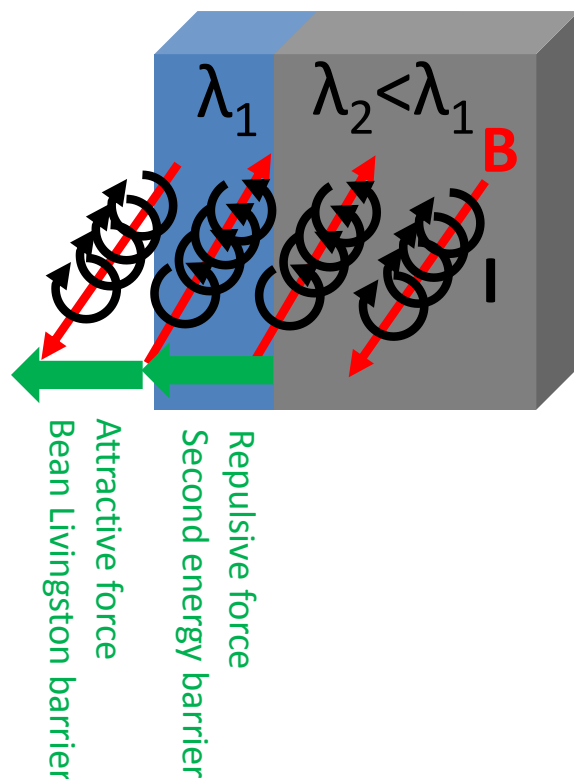


Figure 3: Consider a parallel vortex in a superconductor. To fulfill the boundary conditions at the vacuum superconductor interface an image current is introduced yielding an attractive force to the surface. An energy barrier (Bean Livingston barrier) is built up, which allows the superconductor to remain in a flux free Meissner state above  $H_{c1}$ . At the interface between two superconductors of different penetration depth there is a force on vortices towards the material with larger  $\lambda$ , creating a second energy barrier if  $\lambda_1 > \lambda_2$ .

hand, in a recent publication it was shown that niobium can reach the superheating field if coated with MgB2 or Nb3Sn even for a DC field [23]. The results have been interpreted that there is a second surface barrier at the interface between the two superconductors if  $\lambda_2 < \lambda_1$  as theoretically derived by Kubo [14]. This effect is visualized using the concept of image vortices in Fig. 3. The reason why only the boundary between the two superconductors and not between surface and vacuum can provide shielding above  $H_{c1}$  can be related to the proximity effect acting between the two superconductors. For details we refer to [23]. Potentially a layer with a larger penetration depth could also push Nb3Sn, NbTiN or other materials such as MgB2 to their superheating field enabling accelerating gradients beyond state of the art of niobium technology.

## ACKNOWLEDGMENT

The  $\mu$ SR measurements were performed at the Swiss Muon Source ( $S\mu S$ ), at the Paul Scherrer Institute in Villigen, Switzerland. The authors would like to thank Sam Posen (Fermilab) and Matthias Liepe, (Cornell) for supplying the Nb3Sn sample. A.-M. Valente-Feliciano's work is supported by the U.S. Department of Energy, Office of Science, Office of Nuclear Physics under contract DE-AC05-06OR23177. The TEM work was performed in part at the Analytical Instrumentation Facility (AIF) at North Carolina State University, which is supported by the State of North Carolina and the National Science Foundation (award number ECCS-1542015). The AIF is a member of the North Carolina Research Triangle Nanotechnology Network (RTNN), a site in the National Nanotechnology Coordinated Infrastructure (NNCI).

## REFERENCES

- [1] T Prokscha, E Morenzoni, K Deiters, F Foroughi, D George, R Kobler, A Suter, and V Vrankovic. The new  $\mu e4$  beam at psi: A hybrid-type large acceptance channel for the generation of a high intensity surface-muon beam. *Nuclear Instruments and Methods in Physics Research Section A: Accelerators, Spectrometers, Detectors and Associated Equipment*, 595(2):317–331, 2008.
- [2] E Morenzoni, H Glückler, T Prokscha, HP Weber, EM Forgan, TJ Jackson, H Luetkens, Ch Niedermayer, M Pleines, M Birke, et al. Low-energy  $\mu$ sr at psi: present and future. *Physica B: Condensed Matter*, 289:653–657, 2000.
- [3] Matthew C Burton, Melissa R Beebe, Kaida Yang, Rosa A Lukaszew, Anne-Marie Valente-Feliciano, and Charles Reece. Superconducting nbtin thin films for superconducting radio frequency accelerator cavity applications. *Journal of Vacuum Science & Technology A: Vacuum, Surfaces, and Films*, 34(2):021518, 2016.
- [4] S. Posen and D.L. Hall. Nb3Sn superconducting radiofrequency cavities: fabrication, results, properties, and prospects. *Superconductor Science and Technology*, 30(3):033004, 2017.

- [5] A. Suter and B.M. Wojek. Musrfit: A Free Platform-Independent Framework for muSR Data Analysis. *Physics Procedia*, 30:69–73, 2012.
- [6] JP Biersack and W Eckstein. Sputtering studies with the monte carlo program trim. sp. *Applied Physics A*, 34(2):73–94, 1984.
- [7] C Poole. *Handbook of superconductivity*. Academic Press, London, 2000.
- [8] Matthias Hein. *"High-Temperature-Superconductor Thin Films at Microwave Frequencies"*. Springer, New York, 1999.
- [9] TP Orlando, EJ McNiff Jr, S Foner, and MR Beasley. Critical fields, pauli paramagnetic limiting, and material parameters of nb 3 sn and v 3 si. *Physical Review B*, 19(9):4545, 1979.
- [10] Anne-Marie Valente-Feliciano. Superconducting rf materials other than bulk niobium: a review. *Superconductor Science and Technology*, 29(11):113002, 2016.
- [11] Lei Yu, Nathan Newman, and John M Rowell. Measurement of the coherence length of sputtered nb/sub 0.62/ti/sub 0.38/n thin films. *IEEE transactions on applied superconductivity*, 12(2):1795–1798, 2002.
- [12] E.H.Brandt. Superconductors in realistic geometries: geometric edge barrier versus pinning. *Physica C: Superconductivity*, 332(1):99–107, 2000.
- [13] T. Kubo, Y. Iwashita, and T. Saeki. Radio-frequency electromagnetic field and vortex penetration in multilayered superconductors. *Applied Physics Letters*, 104(3):032603, 2014.
- [14] T. Kubo. Multilayer coating for higher accelerating fields in superconducting radio-frequency cavities: a review of theoretical aspects. *Superconductor Science and Technology*, 30(2):023001, 2016.
- [15] Tobias Junginger. *Investigations of the surface resistance of superconducting materials*. PhD thesis, University Heidelberg, 2012. submitted 5.6.12.
- [16] M. Tinkham. *Introduction to Superconductivity*. Dover Publications, 2004.
- [17] M.K. Transtrum, G. Catelani, and J.P. Sethna. Superheating field of superconductors within Ginzburg-Landau theory. *Phys. Rev. B*, 83(9), 2011.
- [18] S Posen, N Valles, and M Liepe. Radio frequency magnetic field limits of nb and nb 3 sn. *Physical review letters*, 115(4):047001, 2015.
- [19] T Junginger, W Weingarten, and C Welsch. Extension of the Measurement Capabilities of the Quadrupole Resonator. arXiv:1204.1018v1 accepted for publication in Rev. Scient. Instr., 2012.
- [20] A. Gurevich. Enhancement of RF breakdown field of superconductors by multilayer coating. *Applied Physics Letters*, 88:012511 – 012511–3, 2006.
- [21] Hasan Padamsee, Tom Hays, and Jens Knobloch. *RF superconductivity for accelerators*. Wiley, Weinheim, 2. edition, 2008.
- [22] A. Romanenko. Pathway to high gradients in superconducting rf cavities by avoiding flux dissipation. In Proc. EPAC2018, paper WEYGBF2, Vancouver, Canada, May 2018.
- [23] T Junginger, W Wasserman, and RE Laxdal. Superheating in coated niobium. *Superconductor Science and Technology*, 30(12):125012, 2017.